Chromosoma (2000) 109:266–279

CHROMOSOMA

Non-apoptotic chromosome condensation induced by stress: delineation of interchromosomal spaces

Debora Plehn-Dujowich[1], Peter Bell[1], Alexander M. Ishov[1], Chris Baumann[2], Gerd G. Maul[1]

[1] The Wistar Institute, 3601 Spruce Street, Philadelphia, PA 19104, USA
[2] Laboratory of Receptor Biology and Gene Expression, National Cancer Institute, Bethesda, MD 20892, USA

Received: 26 November 1999 / Accepted: 29 February 2000

Abstract. Chromosomes are known to occupy distinct territories, suggesting the existence of definite borders. Visualization of these borders requires chromatin condensation like that seen in prophase cells. We developed a novel method to induce chromosome condensation in all cells regardless of cell cycle stage using a complex set of stresses. The cells were not apoptotic, as indicated by the absence of DNA damage, maintenance of the intact lamina and scaffold attachment factor A, and by the continuation of metabolic processes as well as proliferative capacity. That the appearance of chromosome condensation did not represent a premature mitotic event was shown by the absence of fibrillarin and Ki67 envelopment of chromosomes, continued protein synthesis and the reversibility of chromosome condensation. That chromosome condensation was achieved was demonstrated by the removal of chromatin from the nuclear envelope and chromosome painting. Specific genetic sites known to be at the surface of chromosomes retained their positions as shown by in situ hybridization. Stress-induced chromosome condensation was used to prove that specific nuclear domains such as ND10 are interchromosomally located and that green fluorescent protein-tagged ND10-associated proteins are useful markers for chromosomal boundaries after adenovirus 5 track formation in vivo. From these observations we conclude that chromosomal territories appear to have boundaries that exclude developing macromolecular aggregates.

Introduction

In the interphase nucleus of cultured cells chromatin appears rather homogeneously dispersed with the exception of heterochromatin, which is often found at the nucleolus and associated with the nuclear envelope. However, this apparent homogeneity is deceiving, as the individual chromosomal spaces have been identified as distinct chromosomal territories using chromosome painting techniques (Cremer et al. 1988; Lichter et al. 1988; Pinkel et al. 1988). Recently, chromosomal territories have been shown to have a nonrandom distribution (Nagele et al. 1999). In addition, the interchromosomal spaces that have been delineated at the light microscopic level, known as “speckles” (Spector et al. 1983; Spector 1984, 1990; Nyman et al. 1986; Verheijen et al. 1986), correspond to the previously ultrastructurally identified interchromatin granule clusters (Fakan and Puvion 1980). Recently, interchromosomal spaces in live cells have been identified by green fluorescent protein (GFP)-tagged splicing factors showing large-scale movement that changes our perception of nuclear space interactions (Misteli and Spector 1998). In addition, nuclear-targeted vimentin has been shown to outline the chromosomal boundaries (Bridger et al. 1998). If such interchromosomal spaces were significant for nuclear processes, it would be desirable to be able to observe them in vivo. The resolution limit of the light microscope is not sufficient to permit the observation of the potential movement of GFP-tagged proteins or otherwise fluorescently labeled components, although diffusion of poly(A) throughout the interchromatin space has been investigated by hybridizing with caged fluorescein-labeled poly(T) (Politz et al. 1999). Premature chromosome condensation separates the chromosomal territories but most metabolic processes shut down as when mitotic events unfold (Hittelman and Rao 1976; Rao et al. 1977; Ross 1997).

Chromatin condensation also takes place during apoptosis. There, a complex series of signaling events triggers an enzymatic cascade that affects the nuclear structure through the cleavage of scaffold attachment factor A (SAF-A) by caspases (Gohring et al. 1997), the breakdown of lamin B, and chromatin condensation. Slightly later, DNA fragmentation into oligonucleosomes occurs. The same signaling events have different effects on different cells in the same culture, as they enter apoptosis at quite different rates and some cells survive while others

Edited by: E.R. Schmidt

Correspondence to: G.G. Maul
e-mail: maul@wistar.upenn.edu

succumb. Thus, apoptotic events may be initiated in all cells, but different cells have varying abilities to short circuit the apoptotic cascade. In fact, the fate of a given cell is determined by the integration of multiple pro-apoptotic and anti-apoptotic signals (Jarpe et al. 1998). Apoptosis has been found by many investigators to be intimately linked to cellular proliferation (for review see Meikrantz and Schlegel 1995), and the position of a cell in the cell cycle often determines whether the cell undergoes apoptosis or not.

We show here that a certain set of stresses can induce chromosome condensation in an entire cell population without mitotic shutdown of metabolic activity or delayed death. This chromosome condensation is evidenced by chromosome painting and by confirming the localization of chromosomal components previously defined as internal, surface located or extrachromosomal. We demonstrate that adenovirus 5 (Ad5)-induced track formation of nuclear proteins outlines chromosomal boundaries in the normal nucleus and that the same and other proteins redistribute into the interchromosomal spaces created by stress induction, suggesting that these proteins are relegated to a region distinct from the chromosomal space.

Materials and methods

Antibodies and cell culture

ND10 were visualized using various antibodies. Monoclonal antibody (mAb) 138 appears to recognize an M_r 55,000 protein (NDP55) from human epidermoid (HEp-2) cells and stains ND10 (Ascoli and Maul 1991; Maul et al. 1995). Monoclonal antibody 1150 recognizes Sp100 (Maul et al. 1995) and demonstrates the ND10 pattern in uninduced cells (Epstein 1984). Monoclonal antibody 5E10 recognizes PML (Stuurman et al. 1992; Maul et al. 1995). Rabbit antibodies against Sp100 and rabbit antibodies against PML were obtained from Dr. J. Frey (Korioth et al. 1996). Monoclonal antibodies against the non-snRNP (small nuclear ribonucleoprotein) splicing component SC35 were from Fu and Maniatis (1990). Human antibody 503 recognizes histones, and human antibody 693 recognizes centromeres. Human antibody 21 stains fibrillarin (Yasuda and Maul 1990), and human antibody 44 stains lamin B (Schatten et al. 1985). HEp-2 carcinoma cells were maintained in modified Eagle's medium supplemented with 10% fetal calf serum. All cells were grown at 37°C in a humidified atmosphere of 5% CO_2. For immunofluorescence, cells were grown on round coverslips in 24-well plates or 33 mm petri dishes (Corning Glass, Corning, NY).

Heat shock and stress-induced chromosome condensation (SICC)

Exponentially growing HEp-2 cells on round coverslips in 33 mm plastic petri dishes were used 1 or 2 days after plating when they reached approximately 80% confluency. Petri dishes were sealed with Parafilm to maintain humidity, and floated for 30 min or more in a water bath at 41°C, to retain intact ND10, or at 42°C or above for the dispersion of ND10 proteins. To achieve SICC, heat shock was carried out as described above, but with 0.25 ml of medium, which is sufficient to cover the cells, instead of the customary 2 ml. When specified, cells were incubated with 1000 U/ml of β-interferon (Sigma Chemical Company, St. Louis, Mo.) for 16 h prior to heat shock.

Immunofluorescence microscopy

HEp-2 cells were fixed on ice for 15 min with freshly prepared 1% paraformaldehyde (PFA) in KM buffer (10 mM MES, 10 mM NaCl, 1.2 mM $MgCl_2$, 2.5% glycerol, 0.6 mM phenylmethylsulfonyl fluoride). After washing with PBS, the cells were permeabilized for 20 min on ice with 0.2% Triton X-100 (Sigma) in PBS. Nuclear antigen localization was determined after incubation of permeabilized cells with human autoimmune serum, rabbit antiserum, or mAb diluted in PBS for 1 h at room temperature. Fluorescein- or Texas Red-conjugated secondary antibodies (Vector, Burlingame, Calif.) diluted in PBS were incubated with the cells for 30 min at room temperature, stained for DNA with 0.5 µg/ml of bisbenzimide (Hoechst 33258, Sigma) in PBS, and mounted with Fluoromount G (Fisher Scientific, Pittsburgh, Pa.). Staining with propidium iodide (1 µg/ml, Sigma) in the presence of RNase A (10 µg/ml, Sigma) was carried out in select experiments. Fluorescence images were recorded using a Leica confocal scanning microscope or the Leitz Fluovert inverted microscope.

Fluorescence in situ hybridization (FISH)

After induction of SICC, cells were fixed in 4% PFA in PBS (10 min at room temperature) or, when FISH was combined with immunocytochemistry, subjected to a first step of immunostaining as described above and subsequently refixed in 4% PFA (Ishov et al. 1997). After washing in PBS and equilibrating in 2×SSC, the specimens were dehydrated in an ethanol series (70%, 80% and 100% for 3 min each at –20°C) and air-dried. (1×SSC is 0.15 M NaCl, 0.015 M sodium citrate.) The midsatellite sequence at 1p36 (Buroker et al. 1987), which is preferentially located at the periphery of the chromosomal domain (Kurz et al. 1996), was detected using the biotinylated probe D1Z2 (Oncor, Gaithersburg, Md.). Painting probes specific for chromosomes 1 or 2, which were directly labeled with fluorochromes, were obtained from Vysis (Downers Grove, Ill.). Probes were either diluted 1:20 in 65% formaldehyde, 10% dextran sulfate in 2×SSC (D1Z2), or 1:10 in a mixture of 2 volumes of water and 7 volumes of the hybridization buffer supplied by the manufacturer (Vysis). After applying the probe solution, cellular and probe DNA were simultaneously denatured by heating the specimens at 90°C for 4 min. Hybridization was carried out overnight at 37°C followed by washing with 50% formaldehyde, 2×SSC at 45°C (20 min) and with 2×SSC at 37°C (10 min). For detection of biotinylated probes, cells were incubated for 30 min in fluorescein isothiocyanate (FITC)-avidin (Vector Laboratories, Burlingame, Calif.) diluted 1:500 in 4×SSC with 0.5% BSA. Signals were amplified with biotinylated anti-avidin (Vector, 1:250 in 4×SSC with 0.5% BSA) for 30 min followed by another round of FITC-avidin staining. Between each step, specimens were washed three times in 4×SSC and once in 4×SSC with 0.1% Tween for 3 min each. Cells were photographed using a Leitz Fluovert inverted microscope. Every cell was photographed twice: once with only Hoechst labeling, and once with simultaneous labeling of the DNA with Hoechst and the FISH signal. The distribution of ND10, the D1Z2 locus and centromeres with respect to the chromatin was determined, and the Hoechst labeling intensity at the location of each structure was quantitated on the photograph where Hoechst labeling alone was used. Adobe Photoshop software assigned arbitrary intensity units for every site, and the results were summarized as histograms. For each type of structure, 100 localization points were chosen and corresponding Hoechst intensities were determined.

Assessment of DNA fragmentation

HEp-2 cells were grown on 33 mm petri dishes until 80% confluent. After induction of SICC at 41°C for 30 min as described above, the cells were returned to normal growth conditions for a recovery period of 0, 6 or 24 h. The cells were trypsinized and re-

suspended in 1 ml of DMEM, 10% FBS. The cell suspension was centrifuged at 2000 rpm in an Eppendorf tabletop centrifuge for 5 min. The supernatant was discarded, and 28 µl of lysis buffer (20 mM EDTA, 100 mM TRIS, pH 8, 0.8% SDS) was added to the pellet. RNase A (5 U, Ambion) was added, and the lysate was incubated for 1 h at 37°C. Proteinase K was added to the lysate (200 µg, Sigma), and the mix was incubated at 50°C for 90 min. Loading buffer was added to the samples, and equal amounts of DNA were run on a 1% agarose gel. The gel was stained with ethidium bromide, and the DNA was visualized with a UV illuminator.

Growth curve and clonogenic survival assay

HEp-2 cells were subjected to the 30 min SICC protocol at 41°C, and returned to normal growth conditions. Periodically, the cells were trypsinized, stained with trypan blue, and the number of live cells was determined for duplicate plates. The growth of the cells was monitored in this way for up to 6 days, after which the cells became confluent and the experiment was stopped. Similarly treated cells were plated in duplicate so that the growth of individual cells into colonies could be followed. After 1 week, the number of colonies containing more than five cells was determined, and the results were normalized to plating efficiency. The plating efficiencies of the cells were between 50% and 70%.

In vivo labeling of cells and SDS-polyacrylamide gel electrophoresis (SDS-PAGE) of radiolabeled proteins

After the induction of SICC, the cells were returned to normal growth conditions, with 2 ml of medium per 33 mm petri dish, in a 37°C incubator with a 5% CO_2 atmosphere. After 1 h, the cells were incubated with 40 µCi per dish of ^{35}S-methionine in methionine-free medium for 30 min. The cells were then lysed in cell dissociation buffer (10 mM TRIS, pH 8, 250 mM NaCl, 0.5% Triton X-100, 0.5% sodium deoxycholate, 0.1% SDS) and sheared with a 28-gauge needle and syringe. Lysate (10 µl) was mixed with 10 µl protein loading buffer, and 10 µl of each sample was run on a polyacrylamide/SDS gel of the desired percentage with Kaleidoscope size markers (Biorad) before autoradiography.

Immunoblot analysis

Cell lysates were thawed on ice and sheared with a 28-gauge needle and syringe. Lysate (15 µl), corresponding to an equal number of cells from each sample, was mixed with 5 µl protein loading buffer, and 20 µl of each sample was run on a 7% polyacrylamide/SDS gel with Kaleidoscope size markers (Biorad). Immunoblotting was carried out as previously described (Plehn-Dujowich and Altman 1998), using polyclonal antibodies against SAF-A (Gohring et al. 1997) and horseradish peroxidase-linked goat anti-rabbit IgG secondary antibodies from Vector (Burlingame, Calif.). To visualize the desired proteins, blots were incubated with the chemiluminescence substrate from the ECL kit (Amersham, Arlington, Ill.) according to the manufacturer's protocol.

Green fluorescent protein-PML inducible cell line

The inducible GFP-PML cell line was established based on the episomal version of the tetracycline-regulatable two-plasmid system (Jost et al. 1997). The HeLa Tet-Off cell line expressing the Tet repressor fused to Vp16 was purchased from Clontech (Palo Alto, Calif.). Human PML was initially cloned into the pEGFP-C1 plasmid (Clontech) downstream of the GFP coding sequence, and the PML-GFP fusion was re-cloned into pCEPTetP containing the Tet repressor binding site fused to the min CMV (cauliflower mosaic virus) promoter. Nuclear maintenance and replication of this episomal plasmid is controlled by the Epstein-Barr virus (EBV) origin (OriP) and EBV nuclear protein EBNA-1. The plasmid also contains the hygromycin phosphotransferase gene (HygroR) for selection in eukaryotic cells. pCEPTetP-GFP-PML was transfected into HeLa Tet-Off cells using DOSPER reagents (Boehringer-Mannheim) according to the manufacturer's recommendations. Transfected cells were selected using 200 µg/ml hygromycin B and 2 µg/ml of tetracycline. After the end of the selection process, PML expression was activated by tetracycline removal and monitored by immunoblot analysis and direct observation in the fluorescence microscope.

Adenovirus infection

HEp-2 cells were grown on glass coverslips in 33 mm petri dishes until 80% confluent. The cells were treated with 1000 U/ml of β-interferon for 9 h prior to infection to induce the synthesis of ND10 proteins. Cells were infected with the Ad5 802 mutant, which lacks the single strand DNA binding protein, DBP. This mutant was chosen because it creates longer PML tracks than the wild-type virus. At 16 h after infection, the cells were subjected to SICC, and were fixed and stained with Hoechst. PML was detected with rabbit anti-PML antibodies and FITC-conjugated anti-rabbit antibodies. Chromatin was detected with human anti-histone antibodies and Texas Red-conjugated anti-human antibodies. The cells were visualized using the Leica confocal scanning microscope.

Time-course imaging of GFP-PML

For in vivo studies, HeLa cells expressing a GFP-PML fusion protein were grown on glass-bottomed coverslips (MatTek Corp, Ashland, Mass.) in phenol red-free DMEM. Time-course imaging was performed on a DeltaVision imaging system (Applied Precision, Wash.) utilizing an Olympus IX70 inverted microscope equipped with a 63× (1.4 NA) oil immersion objective. The temperature was maintained at 37°C with a NevTek Air Stream stage incubator (NevTek, Burnsville, Va.). Prior to imaging, the medium was supplemented with 10 mM HEPES, pH 7.4 to maintain physiological pH during the time of the experiment. Images were taken every 20 s for 2–3 h. The resulting time series was then projected as an *xyt* plot and rotated 90 degrees to enable the *x* and *y* translation of a particular ND10 to be observed as a function of time.

Results

Redistribution of ND10 proteins after heat shock

Cells respond to various stresses differentially and each type of stress may have different effects depending on its intensity. To achieve controlled nuclear morphological changes we varied several stresses, beginning with heat shock. Heat shock leads to the dispersion of several proteins normally concentrated in ND10 (Maul et al. 1995). We studied the redistribution of three ND10-associated proteins in HEp-2 cells, and found that the effect of heat shock on the dispersion of each protein was different. Under normal conditions, an average of ten brightly staining ND10 were visible in each cell (Fig. 1A). After 30 min exposure to elevated temperatures, Sp100 was the first ND10 protein to be redistributed throughout the nucleus at 43°C from the domains of high concentration (Fig. 1B). Sp100 was no longer detectable at higher temperatures, whereas PML staining retained its microdot

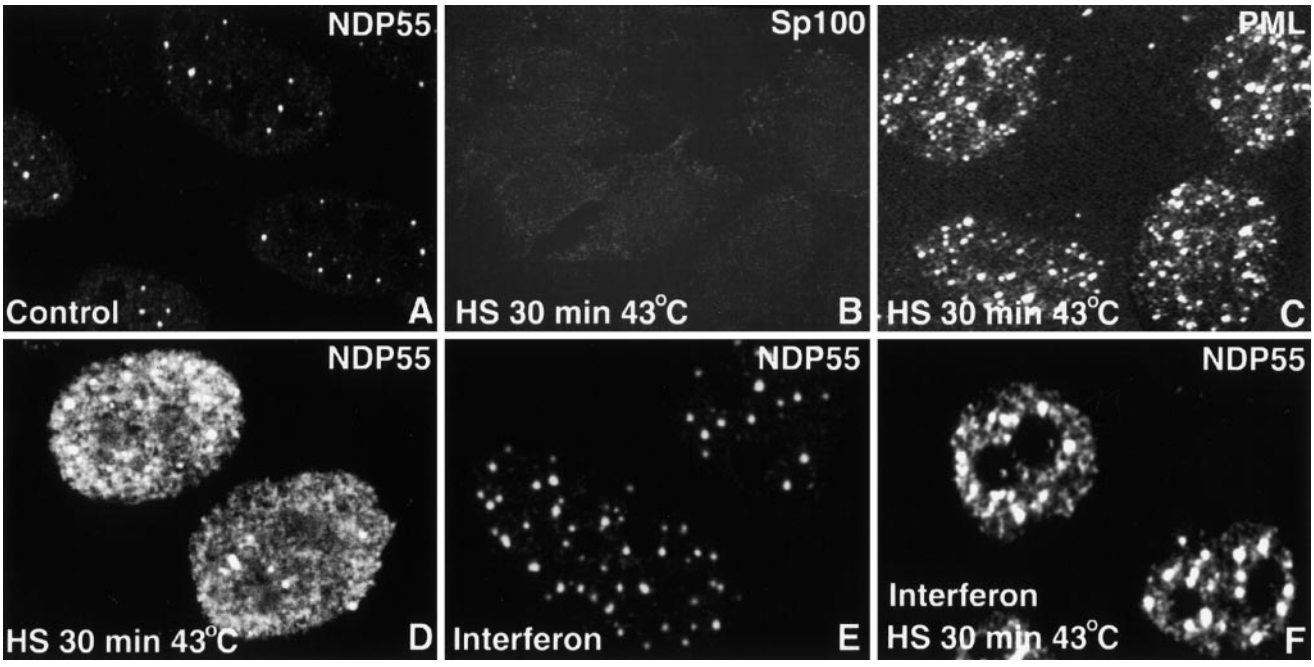

Fig. 1A–F. Heat shock induces redistribution of ND10 antigens. A heat shock (*HS*) was applied to different HEp-2 cell cultures by incubation at 43°C for 30 min. **A** Control at 37°C reacted with monoclonal antibody (mAb) 138, which stains NDP55. **B** Cells reacted with mAb 1150, in which the dispersion of Sp100 is induced by heat shock. Exposure was increased to show background staining outlining cells. **C** PML stained with mAb 5E10 after heat shock, retaining its microdot appearance. **D** NDP55 staining increased with heat shock throughout the nucleus. **E** Incubation of the cells with β-interferon 16 h prior to staining increases the number of ND10 in the nucleus, as shown by labeling with mAb 138. **F** Treatment with β-interferon 16 h prior to heat shock inhibits the dispersal of ND10. Staining for NDP55 shows the presence of a large number of intact ND10, together with diffuse nucleoplasmic staining

appearance even after 30 min exposure at 43°C (Fig. 1C). With heat shock NDP55 staining increased throughout the nucleus, and the protein became dispersed only after heating at temperatures higher than 43°C (Fig. 1D). Staining with either the Hoechst DNA intercalating dye or propidium iodide revealed no change in the chromatin distribution at the end of the temperature elevations.

Interferon treatment is known to up-regulate the expression of ND10 proteins, which in the case of PML should lead to apoptosis (Quignon et al. 1998). We decided to investigate whether preincubation of the cells with β-interferon combined with heat shock would have any effect on the distribution of ND10-associated proteins or on apoptosis as defined by modification of chromatin distribution. We found that incubating the cells with β-interferon overnight, prior to heat shock, prevented the complete dispersion of the ND10 proteins (Fig. 1E, F), indicating that interferon conveys some protection against this particular stress response. No chromatin condensation was found nor did we recognize any apoptotic cells at the end of the treatment or 24 h later.

A combination of stresses results in chromosome condensation

Heat shock at high temperatures (45°C) is known to induce apoptosis (Li et al. 1996; Li and Franklin 1998), resulting in complete chromatin condensation. We decided to investigate different conditions under which to induce chromatin condensation without provoking apoptosis of the cells. We tested the effect on the cell of a radical reduction of nutrients by removing most of the medium, leaving just enough to cover the cell with a thin film of medium. After fixation and staining with Hoechst, chromosome condensation was observed, although this effect was not very reproducible at 37°C. However, when these experimental conditions were combined with heat shock at 42°C for 30 min, an advanced chromatin condensation was observed that resembled the formation of individual chromosomes in all cells in the culture dish (Fig. 2A, B; Fig. 3A). Thus, mild heat shock at 42°C and deprivation of medium result in SICC.

We tried to define the minimal stress necessary for the full development of the effect of SICC. First, we reduced the temperature and found that the full effect was achieved at 41°C. At this heat-shock level ND10 were retained and none of the ND10-associated proteins dispersed. We could, therefore, define the spaces where ND10 are located. As shown in Fig. 3A, ND10 are located in the interchromosomal spaces. At 43°C, ND10 became dispersed and the ND10 proteins were distributed throughout the interchromosomal spaces (Fig. 3B). Secondly, we tested the length of time the combined stress treatment at 41°C needed to be applied. We found that time intervals as short as 15 min can result in SICC if the condition is allowed to develop at normal levels of medium at 37°C. However, complete chromosome con-

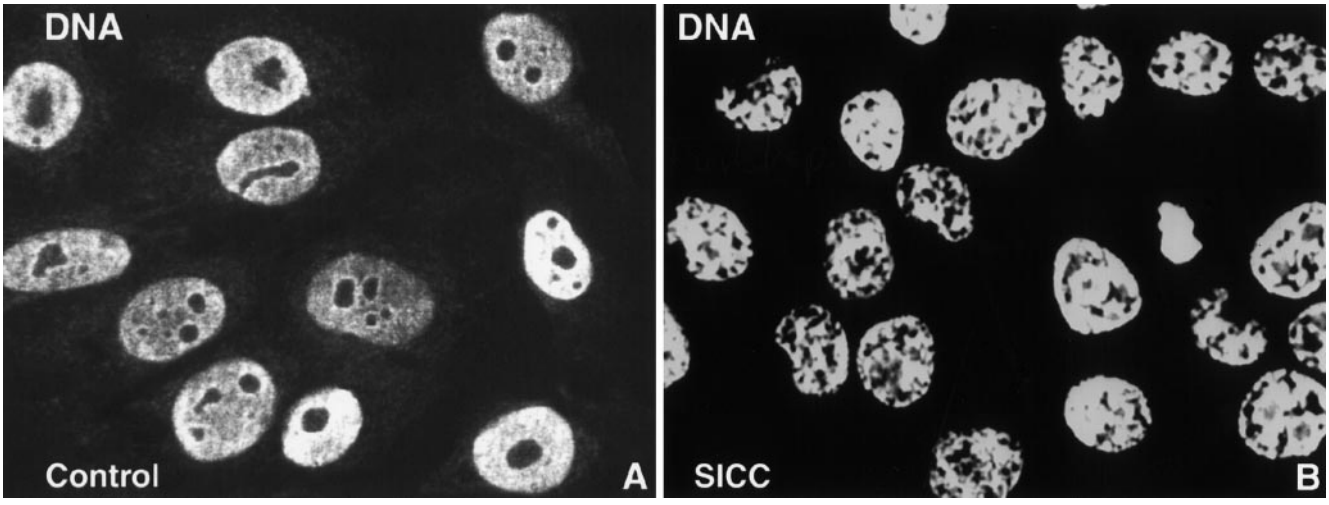

Fig. 2A, B. Mild heat shock and deprivation of medium result in stress-induced chromosome condensation (*SICC*) **A** Control HEp-2 cells stained with Hoechst 33258. The chromatin is uniformly dispersed in the nucleus. **B** Cells were heated at 42°C for 30 min and maintained in reduced amounts of medium, resulting in SICC. The chromatin, stained with Hoechst, is visibly condensed as if the cells were all in prophase

densation of all cells was best achieved at longer times and 30 min at 41°C was adopted as a standard procedure to induce SICC.

Two aspects of the low medium levels are noteworthy: a massive pH shift and higher gas exchange at the cell surface. Measurement of the pH of the medium before and after the stress treatment revealed an increase in the pH from 7 to 10. In a follow-up experiment we increased the pH level to 10 in the presence of a normal amount of medium and found that heat shock together with an increase in pH alone was insufficient to induce SICC (data not shown). Increasing the interferon-induced proteins by exposure of the cells to 1000 U/ml β-interferon had no effect on SICC (data not shown).

SICC does not lead to apoptosis or necrosis

One of the hallmarks of apoptosis is the condensation and cleavage of chromatin (Sellins and Cohen 1987; Harmon et al. 1990). During the late stages of apoptosis, the chromatin condenses while remaining membrane bound, and the DNA is cleaved to multiples of nucleosomal lengths of 180–200 nucleotides. To compare the stress-induced SICC with apoptosis, we irradiated HEp-2 cells with UV light for 3 min. This induced apoptosis, with its concomitant chromatin condensation. The DNA of the cells was stained with propidium iodide, and PML was labeled for immunofluorescence with rabbit anti-PML antibodies. As shown in Fig. 3A, the appearance of the chromatin after SICC is very different from that of apoptotic cells (Fig. 3C). The former is composed of chromatin strands that resemble chromosomes, whereas the latter is composed of condensed spherical bodies. It is interesting to note that PML in ND10 remained intact in apoptotic cells, and ND10 were excluded from the clumped chromatin. To determine whether DNA cleavage occurred during SICC,

Fig. 3A–P. Distribution of nuclear antigens and genetic loci in HEp-2 cells after SICC. Cells were visualized by scanning confocal microscopy and the chromatin was stained with propidium iodide in **A–L**. In **M–P**, DNA was stained with Hoechst 33258 and documented with an inverted microscope. **A** Cells were heated at 41°C for 30 min with reduced amounts of medium (*stress*), resulting in SICC. Under these conditions of lower heat shock, ND10 remained intact, as shown by staining with rabbit anti-PML antibodies, and were shown to be located in the interchromosomal spaces. **B** When SICC is induced at the higher temperature of 43°C, ND10 disperse, and PML staining is located throughout the interchromosomal spaces. **C** Apoptosis induced by 3 min of UV treatment; chromatin is completely condensed into spherical bodies. **D** Cells infected with the adenovirus 5 (Ad5) 802 mutant 12 h prior to induction of SICC. The PML tracks were reconstructed from optical sections throughout the nucleus, whereas the chromatin was photographed from one confocal section to reduce the contribution of the nuclear surface-associated chromatin. **E** In control cells, lamin B forms a ring around the chromatin. **F** After SICC, the lamina is retained, but the condensed chromatin is slightly detached from the nuclear envelope. **G** Control cells stained with human anti-fibrillarin antibodies; fibrillarin is released from the nucleolus during early prophase and attaches to the surface of the chromosomes. **H** After SICC, fibrillarin is released from the nucleolus into the interchromosomal spaces In the mitotic cell (*lower right*) fibrillarin is excluded from the chromosomal mass. **I** Ki67 stains heterochromatin. In control mitotic cells, Ki67 is found to surround the chromosomes (cell in *center right* of the panel), to be prominent in G1 cells (cells at *top left* and *lower right* of the panel), and to cover the margins of the nucleolus during later steps in the cell cycle (cells at *bottom left* of the panel). **J** Ki67 localized in the interchromosomal spaces after SICC. In mitotic cells (*bottom left* cell), Ki67 is excluded from the chromosomes. **K** The spliceosome assembly factor SC35 is distributed in 30–40 nuclear domains in control cells. **L** After SICC, SC35 seems to redistribute to the interchromosomal spaces, also forming a ring around the chromatin. **M** Chromatin condensation in cells after SICC, visualized with an inverted microscope. **N** After SICC, chromosome painting was carried out using probes specific for human chromosome 1 (*red*) and 2 (*green*). The picture shows that the chromatin condensed into non-overlapping individual chromosomal territories. **O** After SICC, immunocytochemistry was combined with fluorescence in situ hybridization to show the relative positions of ND10 and the D1Z2 locus with respect to the chromatin. **P** Localization of centromeres with respect to the condensed chromatin after SICC

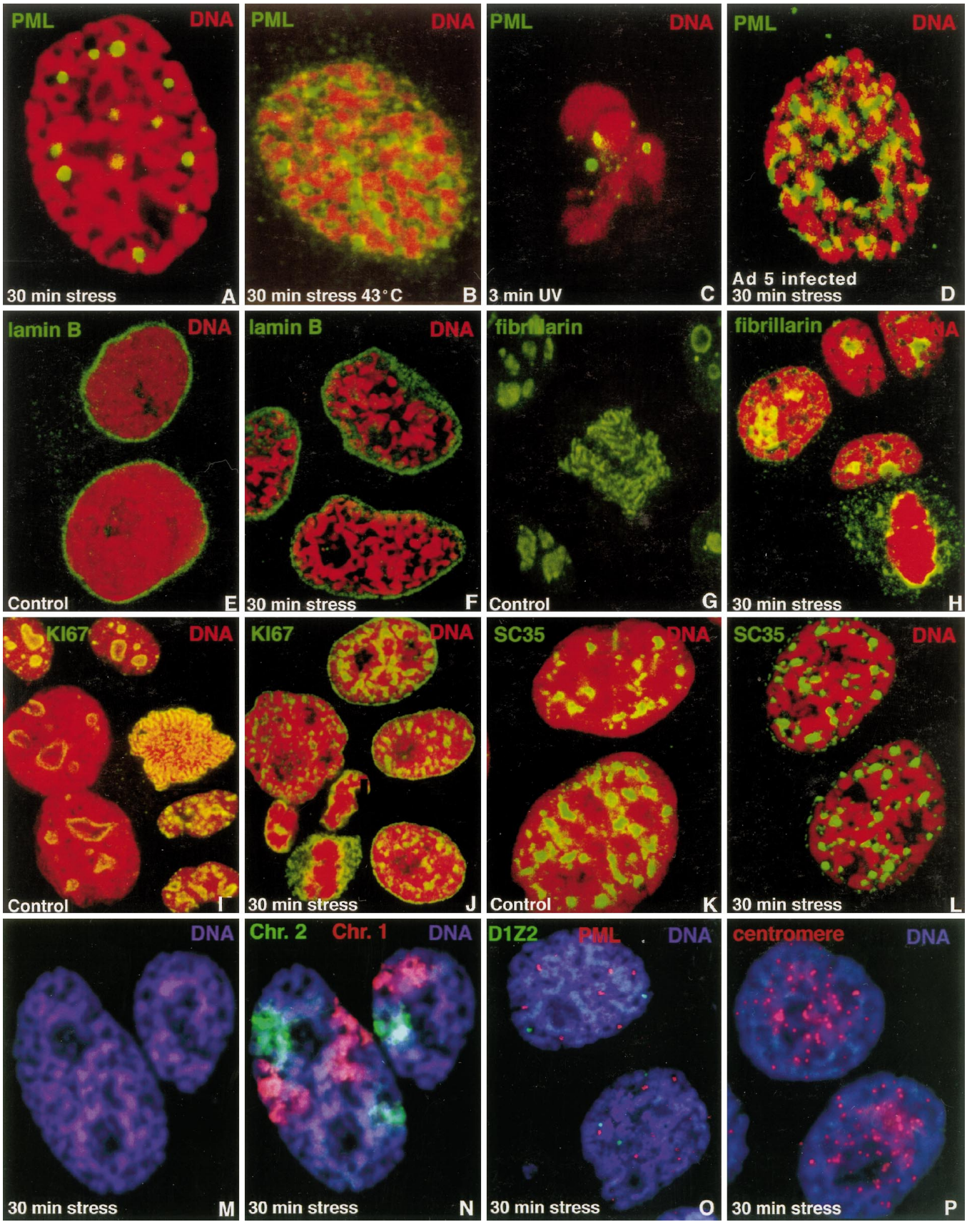
PML DNA
30 min stress A
PML DNA
30 min stress 43°C B
PML DNA
3 min UV C
PML DNA
Ad 5 infected
30 min stress D
lamin B DNA
Control E
lamin B DNA
30 min stress F
fibrillarin
Control G
fibrillarin
30 min stress H
KI67 DNA
Control I
KI67 DNA
30 min stress J
SC35 DNA
Control K
SC35 DNA
30 min stress L
DNA
30 min stress M
Chr. 2 Chr. 1 DNA
30 min stress N
D1Z2 PML DNA
30 min stress O
centromere DNA
30 min stress P

genomic DNA was isolated after induction of SICC and a recovery period of 0, 6 or 24 h under normal growth conditions and analyzed by agarose gel electrophoresis. No DNA ladders were found, indicating that SICC did not represent late stages of apoptosis (data not shown).

Since the loss of lamin B had been reported as a consequence of apoptosis (Lazebnik et al. 1993, 1995) as well as of mitosis (Gerace and Blobel 1980), we tested whether lamin B was lost during the stress-induced chromosome condensation. Normal lamin B staining is shown in the control cells in Fig. 3E. As shown in Fig. 3F, the lamina was retained after SICC, but the condensed chromatin had separated from the nuclear envelope, as expected in prophase. Another major component of the nuclear matrix-lamina fraction of the nucleus that had been reported to be cleaved in a caspase-dependent manner is the SAF-A (Gohring et al. 1997). It binds to scaffold attachment regions (SARs) in the DNA and also to RNA. Cleavage results in a loss of DNA-binding ability and the detachment of SAF-A from nuclear structural sites. To investigate whether the cleavage of SAF-A was also involved in the induction of SICC after stress, we carried out an immunoblot for SAF-A on cell lysates of HEp-2 cells that had undergone SICC. SAF-A was not cleaved in these cells (Fig. 4), providing another indication that this stage of apoptosis was not taking place as a result of SICC.

Cells might become necrotic and die owing to the stress treatment received without going through an apoptotic cycle. To confirm that the cells survived SICC, the growth of the cells was monitored for several days. SICC was applied for 30 min at 41°C, cells were returned to normal growth conditions at 37°C, and the number of live cells was periodically determined using trypan blue exclusion as a criterion for viability. As shown in Fig. 5, following a short lag phase, most of the stressed cells were able to recover from the treatment and continue dividing, eventually attaining numbers comparable to those of control cultures.

These results were confirmed by a clonogenic survival assay. The cells were subjected to stress for different lengths of time and given a 1 h recovery period under normal growth conditions. They were then trypsinized, diluted and plated in duplicate, so that the growth of individual cells into colonies could be followed. After 1 week, the number of colonies of more than five cells was determined. As shown in Fig. 6 there was an approximately 3%–14% reduction in clonogenic survival when the stress exposure varied between 15 min and 30 min. Only if the elevated temperature and low medium levels were extended from 45 min to 2 h did the clonogenic survival drop by 23% and 30%, respectively. Therefore, within the 30 min used as the standard assay, most cells continued to divide after exposure to stress and the exhibition of full SICC.

Moreover, when Hoechst staining was carried out 24 h after the cells had been subjected to the stress and then returned to normal growth conditions, the chromatin condensation was found to be completely reversible in most cells. At this time point, about 5% of cells exhibited an apoptotic phenotype. Most of these cells appeared in doublets, suggesting that they were from a par-

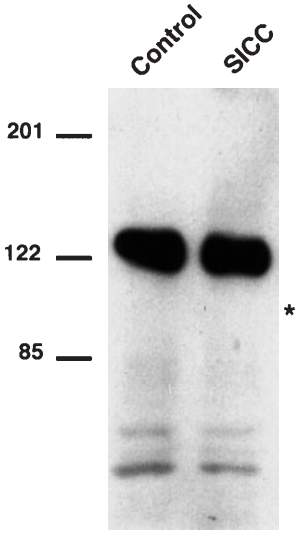

Fig. 4. Immunoblot of scaffold attachment factor A (SAF-A) before and after SICC. The *asterisk* marks the position where the M_r 97,000 cleavage fragment of SAF-A would have been located, if cleavage had occurred

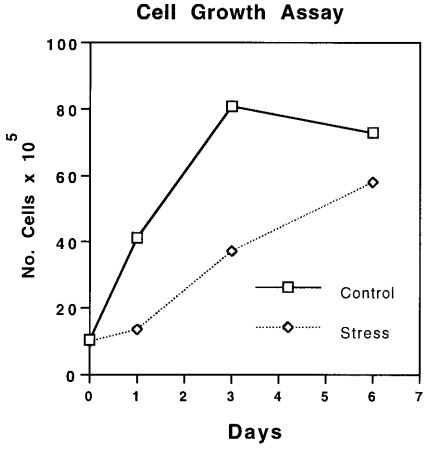

Fig. 5. Growth curve of control cells and cells after SICC. HEp-2 cells were subjected to a 30 min stress at 41°C to induce SICC. They were then returned to normal growth conditions at 37°C. The number of live cells was periodically determined using trypan blue exclusion as a criterion for viability

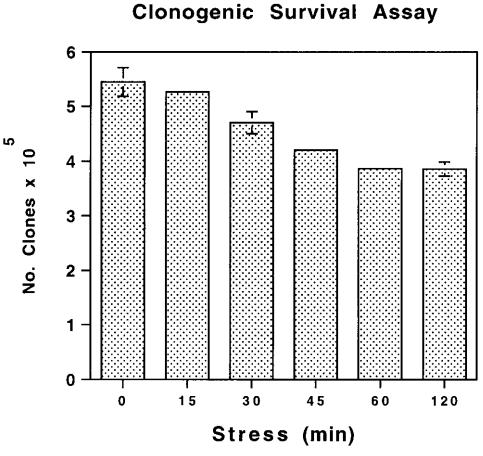

Fig. 6. Clonogenic survival assay of control cells and cells after SICC. HEp-2 cells were subjected to stress at 41°C for different times before being returned to normal growth conditions for 1 h. The cells were then trypsinized, diluted, and plated in duplicate to monitor growth of individual cells into colonies. After 1 week, colonies of more than five cells were counted. *Error bars* indicate the standard error

ticular cell-cycle stage. Based on the size of the cells, their positioning relative to each other, and the shape of the condensed chromatin, we suggest that these cells are post-mitotic or in early G1-phase.

Cells with SICC are not premitotic

The chromatin of cells that have undergone SICC has the appearance of prophase chromosome condensation. As shown above, however, the characteristic lamina breakdown was not observed. We tested whether other changes take place that could be reminiscent of those in prophase. We previously showed that fibrillarin is released from the nucleolus during early prophase and attaches to the surface of chromosomes, finally segregating with the chromosomes (Yasuda and Maul 1990) (Fig. 3G). After SICC, fibrillarin was also released from the nucleolus and appeared to cover the condensed chromatin threads. However, higher resolution suggested that this was not the attachment seen in mitosis, but a release into the interchromosomal spaces (Fig. 3H). In addition, in mitotic cells chromosomes were not covered. On the contrary, fibrillarin was excluded. Similarly, Ki67, a protein considered as a marker for cycling cells, surrounded the chromosomes in control cells, was prominent in G1-phase cells, and covered the margins of the nucleolus later during the cell cycle (Fig. 3I). Like fibrillarin, Ki67 was detected in the interchromosomal spaces after SICC and in the cytoplasm of mitotic cells, excluded from the chromosomes (Fig. 3J). Thus, lamin B, fibrillarin and Ki67 clearly do not display the changes expected from a premitotic cell.

Transcription and protein synthesis are dramatically reduced or shut down during mitosis (Martinez-Balbas et al. 1995; Ross 1997). To determine whether protein synthesis is blocked as a result of SICC, cells incubated with ^{35}S-methionine for 30 min in methionine-free medium after a 30 min stress application were lysed and their proteins were assayed by SDS-PAGE. Similar protein species were synthesized in treated versus untreated cells and synthesis of heat-shock proteins was induced both in heat-shocked cells and in cells subjected to the combined stress of heat shock and medium deprivation, which causes SICC (Fig. 7). This finding indicates that protein synthesis is not substantially inhibited as a result of SICC.

Localization of SC35 after induction of SICC

The spliceosome assembly factor SC35 is distributed in 30–40 nuclear domains (Fig. 3K) that appear to be important for the processing of transcripts (Fu and Maniatis 1990). The localization of SC35 with respect to the chromatin after SICC was studied by immunofluorescence, in conjunction with the visualization of the condensed DNA by propidium iodide staining. In cells having undergone SICC, SC35 domains seemed to redistribute within the interchromosomal spaces during the stress treatment, with formation of a ring between the chromatin and the nuclear envelope (Fig. 3L). This distribution

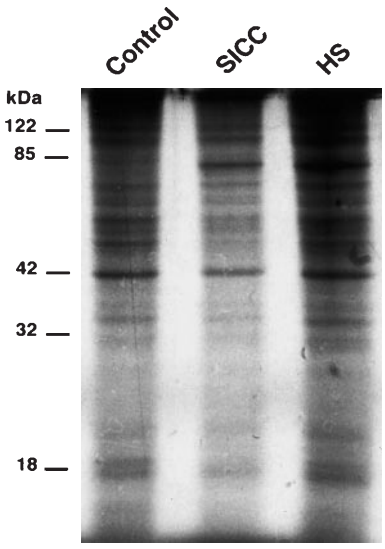

Fig. 7. Protein synthesis continues during SICC. After SICC, HEp-2 cells were incubated with ^{35}S-methionine for 30 min in methionine-free medium. Similar protein species were synthesized in treated versus untreated cells, and heat-shock (*HS*) protein synthesis (hsp70, M_r 70,000) was induced in cells that had undergone heat shock alone or SICC

differs dramatically from the clumped appearance when RNA synthesis is blocked by inhibitors or by heat shock (Spector et al. 1991).

Stress-induced strands of chromatin resemble chromosomes

To determine whether the observed condensation of chromatin into thick strands after stress represented the emergence of individual chromosomes, chromosome painting was carried out. After the simultaneous staining of chromosomes 1 in red and 2 in green we compared the respective patterns with that of DNA stained with Hoechst. We found that the corresponding color outlined the strands of highest DNA staining of two specific areas, demonstrating that individual chromosomes are condensed as a result of the stress treatment (Fig. 3M, N). It was surprising that the painting of the chromosomes was often most intense at the respective surface of the chromosome. Three-dimensional analysis of interphase cells should be possible with this approach.

The periphery of the chromosome has been defined as the site of various gene loci (Kurz et al. 1996). We therefore tested whether such loci could be found in the DNA at the surface of the chromosomes after SICC. For this localization study we utilized the satellite locus D1Z2 and identified it by FISH. This locus was shown to be preferentially located in the periphery of the chromatin in interphase cells (Kurz et al. 1996). As shown in Fig. 3O, fluorescent signal was detected either on the rim of the nucleus or at areas of low DNA staining after SICC. To ensure that the visual inspection of the Hoechst-stained chromatin corresponded to the rim of the chromosome, we quantitated the position relative to structures found in the interchromosomal

spaces, such as ND10 (Fig. 3O), and those on chromosomes, such as centromeres (Fig. 3P), by measuring the DNA intensity at the level of the respective structure, using Photoshop software. The frequency of localization of the various structures with respect to varying Hoechst intensities was calculated, and the results are summarized in the form of histograms in Fig. 8. The distribution of centromeres was found to be random throughout the DNA intensity range. As expected, no centromeres were located at zero Hoechst intensity, where DNA is absent. However, the highest frequency of D1Z2 loci was found in areas of low DNA content, and most ND10 were found in areas of extremely low or no Hoechst intensity. This confirms our previous observations with the confocal microscope that ND10 are located in the interchromosomal spaces, and suggests that the position of other chromosomal loci is maintained after SICC.

Adenovirus 5-induced protein tracks outline chromosomal territories

The presence of ND10 in interchromosomal spaces suggested that protein accumulations were not randomly deposited but that chromosomal territories represented excluded spaces. The ND10-associated proteins might therefore be used to delineate the interface between these territories. We previously found that Ad5 modifies the position of ND10-associated proteins from a spherical outline into one of curvilinear shape resembling tracks (Doucas et al. 1996) and that the Ad5 802 deletion mutant (deficient in DBP) produces particularly well-developed tracks. We also identified conditions allowing chromosome condensation at temperatures that do not disperse ND10 or the tracks. This allowed us to test whether the tracks were positioned in the interchromosomal spaces or meandered randomly through the chromatin. HEp-2 cells infected for 12 h to establish tracks before induction of SICC were stained for PML and histones to display the localization of tracks and chromatin strands. As shown in Fig. 3D, the Ad5-induced PML tracks were detected in the interchromosomal spaces, suggesting that the tracks, formed before chromosome condensation, lay positioned between chromosomal territories.

Currently, no method exists for labeling the interchromosomal domain in live cells. To observe ND10 localization in live cells, we generated HeLa cell lines expressing GFP-PML. When this tagged PML was induced by removal of tetracycline from the culture medium, it located precisely in specific domains (Fig. 9A). That these domains were the same as ND10 was demonstrated through double labeling with another ND10-associated protein, Sp100 (not shown). Since Ad5-induced PML tracks had been found to delineate the interchromosomal spaces, HeLa cells expressing GFP-PML were infected with the Ad5 802 mutant, revealing the formation of PML tracks in live cells. These fine lines represent the tracks throughout the nucleus of an infected cell after reconstruction from optical sections throughout the rather

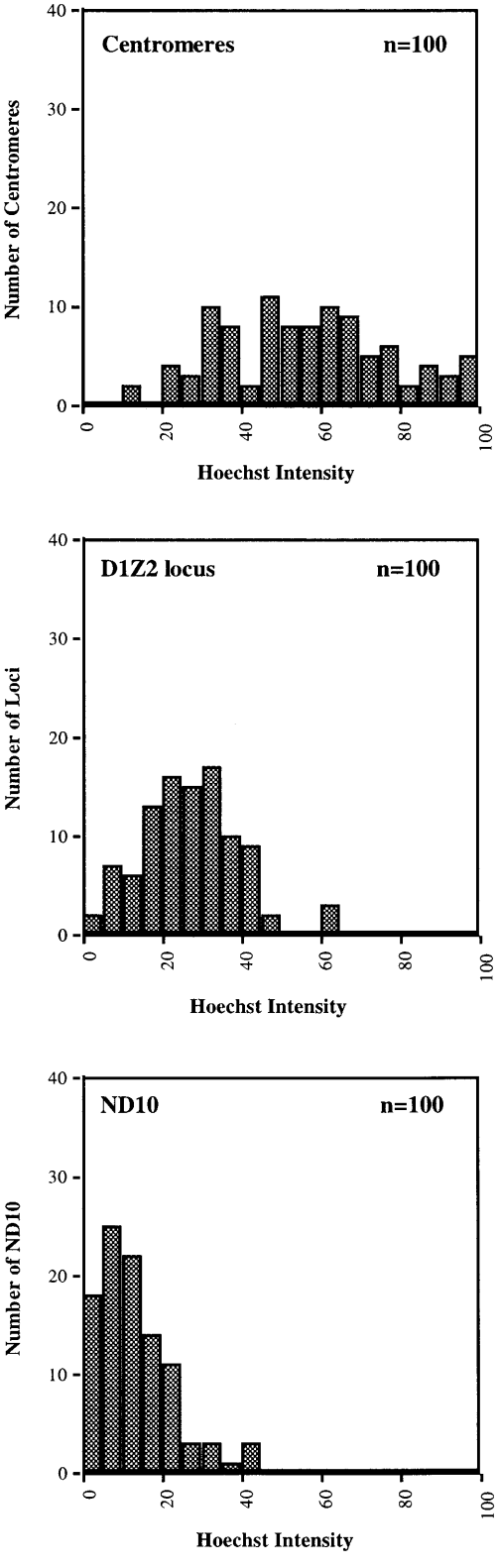

Fig. 8. Distribution of ND10, the D1Z2 locus and centromeres with respect to the chromatin. HEp-2 cells were stressed to induce SICC, and immunocytochemistry was combined with fluorescence in situ hybridization to show the relative position of ND10 (*right panel*), the D1Z2 locus (*center panel*) and centromeres (*left panel*) with respect to the chromatin stained by Hoechst 33258. The number of Hoechst intensities quantitated for each histogram was 100

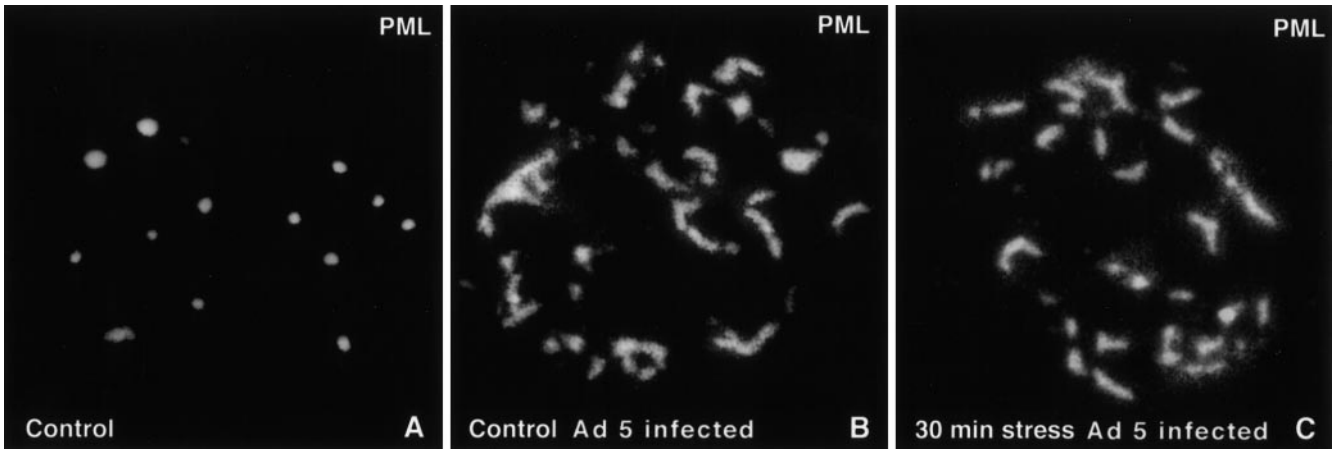

Fig. 9A–C. Green fluorescent protein (GFP)-PML track distribution in live HeLa cells infected with adenovirus. **A** In uninfected control cells GFP-PML localizes to ND10. **B** Control cells infected with the Ad5 802 mutant redistribute GFP-PML into tracks. The image shown is a reconstruction from optical sections through the nucleus of a live cell. **C** Infected cells after SICC. The GFP-PML tracks have the same appearance as in control cells

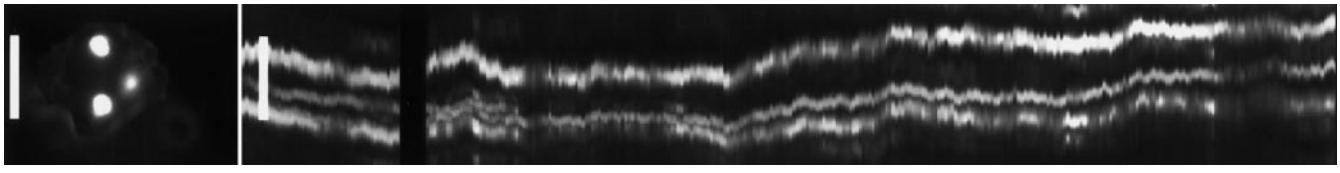

Fig. 10. Temporal distribution of the ND10 domains in living cells. GFP-PML-expressing HeLa cells were visualized by time-course microscopy. Images were taken every 20 s for 25 h yielding 450 images. *Left* time 0. *Bar* represents 5 µm. *Right* all 450 images were layered in an *xyt* projection and rotated 90 degrees along the *x*-axis, displaying a side view of the image. Time 0 is on the *left* and 25 h is on the *right*. *Bar* represents 5 µm

flat nucleus. The tracks formed had the same appearance both in control cells and in cells having undergone SICC (Fig. 9B, C). These results indicate that PML tracks can be used to stain for the interchromosomal spaces in vivo and without the induction of SICC.

To establish whether ND10 are stable structures or are in constant motion along the presumed interchromosomal spaces, time-course microscopy was utilized to study the dynamics of ND10 in live cells. Cells expressing GFP-PML were visualized by digital microscopy and imaged every 20 s for 2–3 h. The resulting time series was then projected as an *xyt* plot and rotated 90 degrees to look at the *x* and *y* translation of particular ND10 as a function of time. Figure 10 shows a representative example of these studies. Here, it is clear that the ND10 do not move significantly throughout the nucleus, indicating that these domains are fixed in position in the uninfected nucleus.

Discussion

Stress-induced chromatin condensation differs from mitosis and apoptosis

We have described a novel phenomenon in mammalian cells: stress-induced chromatin condensation (SICC). A combination of stresses, including heat shock, leads to the condensation of chromatin into chromosome strands, a state superficially resembling prophase before nuclear envelope breakdown. Our investigation of SICC demonstrated that it is different from both mitosis and apoptosis. In fact, the only common phenomenon between the three states was the condensation of the chromatin, although there are differences in the extent to which the chromatin condenses. Apoptosis leads to a complete condensation of the chromatin, with a concomitant loss of nuclear architecture, and mitosis leads to the end-state of condensed chromosomes and nuclear breakdown. Stress-induced chromatin condensation leads to the formation of what appear to be chromosomes, although chromosomal ends as such could not be observed and the nucleus retained its structure. Stress-induced chromatin condensation is also distinct from necrosis because the plasma membrane of cells undergoing SICC remains intact, as assayed by trypan blue exclusion.

The similarities and differences between SICC, mitosis and apoptosis are summarized in Fig. 11. The nuclear membrane disappears in mitosis, but it persists in apoptosis and SICC (Lazebnik et al. 1993). The nuclear lamins disassemble in both mitosis and apoptosis, but not in SICC. The nuclear lamina is solubilized in mitosis as a result of the phosphorylation of the lamin subunits

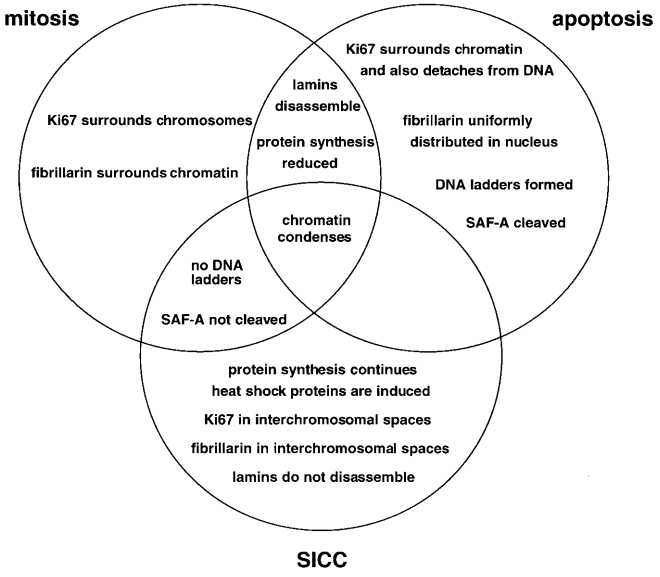

Fig. 11. Relationship between mitosis, apoptosis and SICC

(Gerace and Blobel 1980; Gerace and Burke 1988; Peter et al. 1990). A soluble pool of lamin subunits is available in the cytoplasm for reassembly at the end of mitosis (Gerace and Blobel 1980). Lazebnik and co-workers demonstrated that cells undergoing apoptosis and stained with mAbs against lamins A or B display a diffuse cytoplasmic staining or an undetectable signal (Lazebnik et al. 1993). Contrary to what happens during mitosis, the lamins are apparently degraded in apoptotic cells. In HEp-2 cells having undergone SICC, however, lamin staining was still visible surrounding the nucleus.

Protein synthesis is reduced in both mitosis and apoptosis (Ross 1997). However, we found that after SICC protein synthesis is not noticeably diminished, despite the induction of synthesis of heat-shock proteins. Scaffold attachment factor A is cleaved in apoptosis (Gohring et al. 1997) whereas in mitosis (F.O. Fackelmayer, personal communication) and SICC it remains intact. The DNA is cleaved into nucleosome oligomers in apoptosis, forming a characteristic ladder in agarose gels, whereas no DNA cleavage is observed in mitosis or SICC. Some nuclear antigens behave differently in all three cases. In interphase cells, fibrillarin stains the fibrillar region of the nucleolus and coiled bodies (Reimer et al. 1987). During mitosis, fibrillarin surrounds the chromosomes (Yasuda and Maul 1990), but in apoptosis it becomes distributed uniformly throughout the nucleus (Roy et al. 1992). In SICC, fibrillarin detaches itself from the nucleolus and is positioned in the interchromosomal spaces. The cell cycle marker Ki67, unlike fibrillarin, stains the nucleolar periphery or heterochromatin in interphase cells but also surrounds the chromosomes during mitosis (Verheijen et al. 1989a, b). The authors suggest that Ki67 may be associated with the chromosome scaffold or even form part of it, exerting a function similar to that of topoisomerase II (Verheijen et al. 1989b). In apoptosis, the nuclear structure is lost, and some Ki67 remains attached to the condensed chromatin, while some is detached (Coates et al. 1996). On the other hand, in SICC, Ki67, like fibrillarin, segregates to the interchromosomal spaces. Taking these results into account, we conclude that SICC is a novel phenomenon, distinct from either mitosis or apoptosis.

A type of SICC has previously been described in *Achlya* fungi subjected to heat shock (Pekkala et al. 1984; Pekkala and Silver 1990). Although the chromatin was not visualized by confocal microscopy, the authors observed a marked condensation of the chromatin in electron micrographs, and the DNA became refractory to DNase I digestion during heat shock (Pekkala et al. 1984). The nucleosomal linker-associated histone H1 is involved in the condensation of chromatin in most eukaryotes, but the core histones are also important (McGhee et al. 1980, 1983; Cartwright et al. 1982). The amino-terminal regions of the core histones are necessary for the correct packaging of the chromatin into the 30 nm solenoid structure. The role of the core histones is especially evident in *Achlya* fungi, which lack an H1-like histone and yet are able to undergo chromatin condensation upon heat shock. The chromatin of *Drosophila* also becomes more condensed after heat shock, indicating that this phenomenon may not be restricted to mammalian cells and fungi (Arrigo 1983).

During apoptosis, the chromatin condenses into very dense spheres, which apparently lack any structure. The SAF-A binds to SARs in the DNA, connecting them to the nuclear scaffold, a proteinaceous network. The cleavage of SAF-A in a caspase-dependent manner releases the chromatin from its nuclear attachment sites, leading to the collapse of the chromatin structure. The absence of SAF-A cleavage during SICC may explain why the nucleus retains a large amount of structure, and why the chromatin does not completely condense as it does during apoptosis.

The mechanism by which changes in the cellular environment are relayed to the nucleus to affect chromatin condensation is unknown. Stress-activated protein kinases may sense the heat shock and other stresses in the cell, and may bring about chromatin condensation through a cascade of signals. Stress-induced chromosome condensation may be a checkpoint at which the cell either continues growing or undergoes apoptosis. We noted that after SICC, cells that were already in mitosis or early G1-phase seemed preferentially to undergo apoptosis, consistent with observations in other systems that cycling cells are more likely to undergo apoptosis (King and Cidlowski 1995; Meikrantz and Schlegel 1995; Jarpe et al. 1998). Further study is necessary to determine whether SICC has a protective function for the cell in response to stress. One possible advantage conferred to the cell by SICC would be the reduction of putative DNA replication errors that might result from the stress. In fact, we observed cell-cycle arrest in cells undergoing SICC, resulting in delayed growth.

Interchromosomal position of intact ND10 and dispersed ND10 proteins

Chromosome painting using probes for chromosomes 1 and 2 demonstrated that the thick strands of chromatin formed after SICC represent the emergence of individual chromosomes. Several active and inactive genes, as well as the satellite sequence D1Z2, are preferentially located at the periphery of the chromosomes (Kurz et al. 1996). After SICC, this D1Z2 locus maintained its localization at the periphery of the chromatin, whereas centromere staining revealed the expected random distribution throughout the chromatin. These results indicate that the chromatin retains its orientation after SICC.

A specific relationship between ND10 and chromosomes has previously been inferred from the observation that ND10 may occupy near-symmetrical positions in daughter cells after mitosis (Maul et al. 1996), explainable by spatial memory of the chromosomes in metaphase (Rabl 1885). In addition, several studies have recently shown that chromosomes exhibit preferential positioning in interphase nuclei (Nagele et al. 1999). It has also been shown that several genetic loci occupy predetermined positions in the nucleus during interphase (Marshall et al. 1996; Parreira et al. 1997), and that interphase chromatin is immobile over distances of 0.4 μm (Abney et al. 1997). When HEp-2 cells were subjected to SICC at 41°C, ND10 remained intact and were located interchromosomally. No overlap was seen between ND10 and chromatin. Despite the limit of resolution, ND10 appeared to be attached to the chromosome strands at their periphery and to be rather stable, i.e., they did not move between the chromosomal territories over at least a 2.5 h period. These findings may be construed as indirect evidence for a relationship between the position of ND10 in the nucleus and putative chromosomal attachment sites on the matrix. However, no direct evidence exists at present to indicate whether the position of ND10 in the nucleus is determined by specific chromosomal sites, as has been shown for coiled bodies (Frey and Matera 1995; Smith et al. 1995).

Heat shock by itself induced the dispersion of ND10 proteins. Sp100 dispersed throughout the nucleus at 42°C and was lost at higher temperatures. NDP55 staining increased with heat shock, and became dispersed only after heating to 44°C. However, PML retained its microdot appearance even after heat shock for 30 min at 44°C. Heat shock has been shown to have an effect on the distribution of non-ND10 nuclear proteins, since SC35 splicing domains aggregate in response to heat shock (Spector et al. 1991), probably through inhibition of splicing (Bond 1988). Coiled bodies disperse and form patches in the nucleoplasm (Zirbel et al. 1993; Beven et al. 1995). Heat shock also disrupts the association between snRNPs and coiled bodies (Carmo-Fonseca et al. 1992). A strong heat shock leads to apoptosis, with the concomitant changes in nuclear architecture (Li et al. 1996; Li and Franklin 1998). After SICC was induced at the higher temperature of 43°C, the ND10 protein NDP55 was dispersed and located in the interchromosomal spaces, as was SC35. Thus, SICC has a very different effect from that of heat shock, although elevated temperatures enhance SICC and induce synthesis of heat-shock proteins.

Evidence for interchromosomal spaces

ND10-associated proteins redistributed into lengthy tracks upon infection of cells with adenovirus. We observed particularly well developed tracks in HEp-2 cells infected with an Ad5 mutant that does not replicate owing to the lack of DBP. In cells infected with the Ad5 mutant and subjected to SICC at temperatures that do not cause ND10 protein dispersion, the tracks were found to occupy the interchromosomal spaces. Since the tracks were formed before SICC, the position of the tracks is presumably between the chromosomal territories in normally dispersed chromatin. A similar conclusion was reached through the use of a recombinant cytoplasmic protein, vimentin, engineered to contain a nuclear localization signal (NLS-vimentin) (Bridger et al. 1998). The NLS-vimentin could be induced to form filamentous arrays in the interchromosomal spaces, and colocalized partially with ND10, vimentin RNA and coiled bodies. Interchromosomal protein filaments have also been described in *Drosophila* embryo nuclei (Zimowska et al. 1997), where a Tpr (translocated promoter region) homolog was shown to localize to the interchromosomal domain and to nuclear pore complexes. The findings from such studies suggest that there are spaces between chromosomes or that chromosomal territories have borders that exclude forming aggregates.

Acknowledgements. This study was supported by funds from NIH AI 41136; NIH GM 57599, NIH HD 34612, NSF MCB9728398 and the G. Harold and Leila Y. Mathers Charitable Foundation. NIH Core grant CA-10815 is acknowledged for support of the microscopy facility. D. Plehn-Dujowich was supported by NIH training grant CA09171. We thank F.O. Fackelmayer, J. Frey, N. Stuurman, C. Szostecki, and T. Maniatis for providing the antibodies.

References

Abney JR, Cutler B, Fillbach ML, Axelrod D, Scalettar BA (1997) Chromatin dynamics in interphase nuclei and its implications for nuclear structure. J Cell Biol 137:1459–1468

Arrigo AP (1983) Acetylation and methylation patterns of core histones are modified after heat or arsenite treatment of *Drosophila* tissue culture cells. Nucleic Acids Res 11:1389–1404

Ascoli CA, Maul GG (1991) Identification of a novel nuclear domain. J Cell Biol 112:785–795

Beven AF, Simpson GG, Brown JW, Shaw PJ (1995) The organization of spliceosomal components in the nuclei of higher plants. J Cell Sci 108:509–518

Bond U (1988) Heat shock but not other stress inducers leads to the disruption of a sub-set of snRNPs and inhibition of in vitro splicing in HeLa cells [published erratum appears in EMBO J 7:4020 (1988)]. EMBO J 7:3509–3518

Bridger JM, Herrmann H, Munkel C, Lichter P (1998) Identification of an interchromosomal compartment by polymerization of nuclear-targeted vimentin. J Cell Sci 111:1241–1253

Buroker N, Bestwick R, Haight G, Magenis RE, Litt M (1987) A hypervariable repeated sequence on human chromosome 1p36. Hum Genet 77:175–181

Carmo-Fonseca M, Pepperkok R, Carvalho MT, Lamond AI (1992) Transcription-dependent colocalization of the U1, U2, U4/U6, and U5 snRNPs in coiled bodies. J Cell Biol 117:1–14

Cartwright IL, Abmayr SM, Fleischmann G, Lowenhaupt K, Elgin SC, Keene MA, Howard GC (1982) Chromatin structure and gene activity: the role of nonhistone chromosomal proteins. CRC Crit Rev Biochem 13:1–86

Coates PJ, Hales SA, Hall PA (1996) The association between cell proliferation and apoptosis: studies using the cell cycle-associated proteins Ki67 and DNA polymerase alpha. J Pathol 178:71–77

Cremer T, Lichter P, Borden J, Ward DC, Manuelidis L (1988) Detection of chromosome aberrations in metaphase and interphase tumor cells by in situ hybridization using chromosome-specific library probes. Hum Genet 80:235–246

Doucas V, Ishov AM, Romo A, Juguilon H, Weitzman MD, Evans RM, Maul GG (1996) Adenovirus replication is coupled with the dynamic properties of the PML nuclear structure. Genes Dev 10:196–207

Epstein AL (1984) Immunobiochemical characterization with monoclonal antibodies of Epstein-Barr virus-associated early antigens in chemically induced cells. J Virol 50:372–379

Fakan S, Puvion E (1980) The ultrastructural visualization of nucleolar and extranucleolar RNA synthesis and distribution. Int Rev Cytol 65:255–299

Frey MR, Matera AG (1995) Coiled bodies contain U7 small nuclear RNA and associate with specific DNA sequences in interphase human cells [published erratum appears in Proc Natl Acad Sci USA 92:8532 (1995)]. Proc Natl Acad Sci USA 92:5915–5919

Fu XD, Maniatis T (1990) Factor required for mammalian spliceosome assembly is localized to discrete regions in the nucleus. Nature 343:437–441

Gerace L, Blobel G (1980) The nuclear envelope lamina is reversibly depolymerized during mitosis. Cell 19:277–287

Gerace L, Burke B (1988) Functional organization of the nuclear envelope. Annu Rev Cell Biol 4:335–374

Gohring F, Schwab BL, Nicotera P, Leist M, Fackelmayer FO (1997) The novel SAR-binding domain of scaffold attachment factor A (SAF-A) is a target in apoptotic nuclear breakdown. EMBO J 16:7361–7371

Harmon BV, Corder AM, Collins RJ, Gobe GC, Allen J, Allan DJ, Kerr JF (1990) Cell death induced in a murine mastocytoma by 42–47 degrees C heating in vitro: evidence that the form of death changes from apoptosis to necrosis above a critical heat load. Int J Radiat Biol 58:845–858

Hittelman WN, Rao PN (1976) Premature chromosome condensation. Conformational changes of chromatin associated with phytohemagglutinin stimulation of peripheral lymphocytes. Exp Cell Res 100:219–222

Ishov AM, Stenberg RM, Maul GG (1997) Human cytomegalovirus immediate early interaction with host nuclear structures: definition of an immediate transcript environment. J Cell Biol 138:5–16

Jarpe MB, Widmann C, Knall C, Schlesinger TK, Gibson S, Yujiri T, Fanger GR, Gelfand EW, Johnson GL (1998) Anti-apoptotic versus pro-apoptotic signal transduction: checkpoints and stop signs along the road to death. Oncogene 17:1475–1482

Jost M, Kari C, Rodeck U (1997) An episomal vector for stable tetracycline-regulated gene expression. Nucleic Acids Res 25:3131–3134

King KL, Cidlowski JA (1995) Cell cycle and apoptosis: common pathways to life and death. J Cell Biochem 58:175–180

Korioth F, Maul GG, Plachter B, Stamminger T, Frey J (1996) The nuclear domain 10 (ND10) is disrupted by the human cytomegalovirus gene product IE1. Exp Cell Res 229:155–158

Kurz A, Lampel S, Nickolenko JE, Bradl J, Benner A, Zirbel RM, Cremer T, Lichter P (1996) Active and inactive genes localize preferentially in the periphery of chromosome territories. J Cell Biol 135:1195–1205

Lazebnik YA, Cole S, Cooke CA, Nelson WG, Earnshaw WC (1993) Nuclear events of apoptosis in vitro in cell-free mitotic extracts: a model system for analysis of the active phase of apoptosis. J Cell Biol 123:7–22

Lazebnik YA, Takahashi A, Moir RD, Goldman RD, Poirier GG, Kaufmann SH, Earnshaw WC (1995) Studies of the lamin proteinase reveal multiple parallel biochemical pathways during apoptotic execution. Proc Natl Acad Sci USA 92:9042–9046

Li WX, Franklin WA (1998) Radiation- and heat-induced apoptosis in PC-3 prostate cancer cells. Radiat Res 150:190–194

Li WX, Chen CH, Ling CC, Li GC (1996) Apoptosis in heat-induced cell killing: the protective role of hsp-70 and the sensitization effect of the c-myc gene. Radiat Res 145:324–330

Lichter P, Cremer T, Borden J, Manuelidis L, Ward DC (1988) Delineation of individual human chromosomes in metaphase and interphase cells by in situ suppression hybridization using recombinant DNA libraries. Hum Genet 80:224–234

Marshall WF, Dernburg AF, Harmon B, Agard DA, Sedat JW (1996) Specific interactions of chromatin with the nuclear envelope: positional determination within the nucleus in *Drosophila melanogaster*. Mol Biol Cell 7:825–842

Martinez-Balbas MA, Dey A, Rabindran SK, Ozato K, Wu C (1995) Displacement of sequence-specific transcription factors from mitotic chromatin. Cell 83:29–38

Maul GG, Yu E, Ishov AM, Epstein AL (1995) Nuclear domain 10 (ND10) associated proteins are also present in nuclear bodies and redistribute to hundreds of nuclear sites after stress. J Cell Biochem 59:498–513

Maul GG, Ishov AM, Everett RD (1996) Nuclear domain 10 as preexisting potential replication start sites of herpes simplex virus type-1. Virology 217:67–75

McGhee JD, Rau DC, Charney E, Felsenfeld G (1980) Orientation of the nucleosome within the higher order structure of chromatin. Cell 22:87–96

McGhee JD, Nickol JM, Felsenfeld G, Rau DC (1983) Higher order structure of chromatin: orientation of nucleosomes within the 30 nm chromatin solenoid is independent of species and spacer length. Cell 33:831–841

Meikrantz W, Schlegel R (1995) Apoptosis and the cell cycle. J Cell Biochem 58:160–174

Misteli T, Spector DL (1998) The cellular organization of gene expression. Curr Opin Cell Biol 10:323–331

Nagele RG, Freeman T, McMorrow L, Thomson Z, Kitson-Wind K, Lee H (1999) Chromosomes exhibit preferential positioning in nuclei of quiescent human cells. J Cell Sci 112:525–535

Nyman U, Hallman H, Hadlaczky G, Pettersson I, Sharp G, Ringertz NR (1986) Intranuclear localization of snRNP antigens. J Cell Biol 102:137–144

Parreira L, Telhada M, Ramos C, Hernandez R, Neves H, Carmo-Fonseca M (1997) The spatial distribution of human immunoglobulin genes within the nucleus: evidence for gene topography independent of cell type and transcriptional activity. Hum Genet 100:588–594

Pekkala DH, Silver JC (1990) Characterization and nucleosomal core localization of *Achlya* histones involved in stress-induced chromatin condensation. Exp Cell Res 187:16–24

Pekkala D, Heath B, Silver JC (1984) Changes in chromatin and the phosphorylation of nuclear proteins during heat shock of *Achlya ambisexualis*. Mol Cell Biol 4:1198–1205

Peter M, Nakagawa J, Doree M, Labbe JC, Nigg EA (1990) In vitro disassembly of the nuclear lamina and M phase-specific phosphorylation of lamins by cdc2 kinase. Cell 61:591–602

Pinkel D, Landegent J, Collins C, Fuscoe J, Segraves R, Lucas J, Gray J (1988) Fluorescence in situ hybridization with human chromosome-specific libraries: detection of trisomy 21 and translocations of chromosome 4. Proc Natl Acad Sci USA 85:9138–9142

Plehn-Dujowich D, Altman S (1998) Effective inhibition of influenza virus production in cultured cells by external guide sequences and ribonuclease P. Proc Natl Acad Sci USA 95:7327–7332

Politz JC, Tuft RA, Pederson T, Singer RH (1999) Movement of nuclear poly(A) RNA throughout the interchromatin space in living cells. Curr Biol 9:285–291

Quignon F, De Bels F, Koken M, Feunteun J, Ameisen JC, de The H (1998) PML induces a novel caspase-independent death process [see comments]. Nat Genet 20:259–265

Rabl C (1885) Uber Zellteilung. Morphol Jahrbuch 10:214–330

Rao PN, Wilson B, Puck TT (1977) Premature chromosome condensation and cell cycle analysis. J Cell Physiol 91:131–141

Reimer G, Pollard KM, Penning CA, Ochs RL, Lischwe MA, Busch H, Tan EM (1987) Monoclonal autoantibody from a (New Zealand black × New Zealand white) F1 mouse and some human scleroderma sera target an Mr 34,000 nucleolar protein of the U3 RNP particle. Arthritis Rheum 30:793–800

Ross J (1997) A hypothesis to explain why translation inhibitors stabilize mRNAs in mammalian cells: mRNA stability and mitosis. Bioessays 19:527–529

Roy C, Brown DL, Little JE, Valentine BK, Walker PR, Sikorska M, Leblanc J, Chaly N (1992) The topoisomerase II inhibitor teniposide (VM-26) induces apoptosis in unstimulated mature murine lymphocytes. Exp Cell Res 200:416–424

Schatten G, Maul GG, Schatten H, Chaly N, Simerly C, Balczon R, Brown DL (1985) Nuclear lamins and peripheral nuclear antigens during fertilization and embryogenesis in mice and sea urchins. Proc Natl Acad Sci U S A 82:4727–4731

Sellins KS, Cohen JJ (1987) Gene induction by gamma-irradiation leads to DNA fragmentation in lymphocytes. J Immunol 139:3199–3206

Smith KP, Carter KC, Johnson CV, Lawrence JB (1995) U2 and U1 snRNA gene loci associate with coiled bodies. J Cell Biochem 59:473–485

Spector DL (1984) Colocalization of U1 and U2 small nuclear RNPs by immunocytochemistry. Biol Cell 51:109–112

Spector DL (1990) Higher order nuclear organization: three-dimensional distribution of small nuclear ribonucleoprotein particles [published erratum appears in Proc Natl Acad Sci USA 87:2384 (1990)]. Proc Natl Acad Sci USA 87:147–151

Spector DL, Schrier WH, Busch H (1983) Immunoelectron microscopic localization of snRNPs. Biol Cell 49:1–10

Spector DL, Fu XD, Maniatis T (1991) Associations between distinct pre-mRNA splicing components and the cell nucleus. EMBO J 10:3467–3481

Stuurman N, de Graaf A, Floore A, Josso A, Humbel B, de Jong L, van Driel R (1992) A monoclonal antibody recognizing nuclear matrix-associated nuclear bodies. J Cell Sci 101:773–784

Verheijen R, Kuijpers H, Vooijs P, Van Venrooij W, Ramaekers F (1986) Distribution of the 70 K U1 RNA-associated protein during interphase and mitosis. Correlation with other U RNP particles and proteins of the nuclear matrix. J Cell Sci 86:173–190

Verheijen R, Kuijpers HJ, Schlingemann RO, Boehmer AL, van Driel R, Brakenhoff GJ, Ramaekers FC (1989a) Ki-67 detects a nuclear matrix-associated proliferation-related antigen. I Intracellular localization during interphase. J Cell Sci 92:123–130

Verheijen R, Kuijpers HJ, van Driel R, Beck JL, van Dierendonck JH, Brakenhoff GJ, Ramaekers FC (1989b) Ki-67 detects a nuclear matrix-associated proliferation-related antigen. II Localization in mitotic cells and association with chromosomes. J Cell Sci 92:531–540

Yasuda Y, Maul GG (1990) A nucleolar auto-antigen is part of a major chromosomal surface component. Chromosoma 99: 152–160

Zimowska G, Aris JP, Paddy MR (1997) A *Drosophila* Tpr protein homolog is localized both in the extrachromosomal channel network and to nuclear pore complexes. J Cell Sci 110:927–944

Zirbel RM, Mathieu UR, Kurz A, Cremer T, Lichter P (1993) Evidence for a nuclear compartment of transcription and splicing located at chromosome domain boundaries. Chromosome Res 1:93–106